

Octahedral Coordination of Halide Ions (I^- , Br^- , Cl^-) Sandwich Bonded with Tridentate Mercuracarborand-3 Receptors

Hans Lee, Carolyn B. Knobler, and M. Frederick Hawthorne*

Contribution from the Department of Chemistry and Biochemistry, University of California at Los Angeles, Los Angeles, California 90095-1569

Received March 22, 2001

Abstract: The “anti-crown” *B*-hexamethyl 9-mercuracarborand-3 (**1**) was shown to complex halide ions (I^- , Br^- , Cl^-) in an η^3 -sandwich fashion. Symmetry-allowed interactions of the filled halide ion p-orbitals and the corresponding empty mercury p-orbitals result in three equivalent $p_{Hg}-p_{halide}-p_{Hg}$ three-center two-electron bonds and a sandwich structure. The molecular structures of $[Li \cdot (H_2O)_4][I_2 \cdot I] \cdot 2CH_3CN$, $MePPh_3[I_2 \cdot Br] \cdot ((CH_3)_2CO)_2 \cdot (H_2O)_2$, and $PPN[I_2 \cdot Cl]$ were determined by single-crystal X-ray diffraction studies. Compound $[Li \cdot (H_2O)_4][I_2 \cdot I] \cdot 2CH_3CN$ crystallized in the triclinic space group $P\bar{1}$, $a = 13.312(8)$ Å, $b = 13.983(9)$ Å, $c = 13.996(9)$ Å, $\alpha = 61.16(2)^\circ$, $\beta = 82.34(2)^\circ$, $\gamma = 86.58(2)^\circ$, $V = 4365(2)$ Å³, $Z = 1$, $R = 0.063$, and $R_w = 0.171$. Compound $MePPh_3[I_2 \cdot Br] \cdot ((CH_3)_2CO)_2 \cdot (H_2O)_2$ crystallized in the monoclinic space group $C2/c$, $a = 24.671(8)$ Å, $b = 17.576(6)$ Å, $c = 26.079(8)$ Å, $\beta = 106.424(6)^\circ$, $V = 10847(6)$ Å³, $Z = 8$, $R = 0.0607$, and $R_w = 0.1506$. Compound $PPN[I_2 \cdot Cl]$ crystallized in the monoclinic space group $C2/m$, $a = 37.27(2)$ Å, $b = 29.25(1)$ Å, $c = 10.990(4)$ Å, $\beta = 100.659(7)^\circ$, $V = 11774(8)$ Å³, $Z = 4$, $R = 0.0911$, and $R_w = 0.2369$.

Introduction

The search for macrocyclic multidentate Lewis acid hosts, composed of two or more Lewis acidic centers, is a rapidly expanding endeavor with applications in catalysis,¹ supramolecular self-assembly,² sensors,³ and molecular recognition.^{4–7} Mercuracarborands, cyclic multidentate Lewis acids composed of alternating units of carborane cages and mercury atoms, serve as chelating ligands that simultaneously coordinate halide ion(s) while maintaining their formal -1 oxidation state.^{4,8} Cyclic pentameric $[(CF_3)_2CHg]_5$ coordinates two halide anions (Cl^- , Br^- , I^-) which bind above and below the cavity center.^{9,10} Similarly, tetrameric 12-mercuracarborand-4 ($C_2B_{10}H_{10}Hg_4$) also binds two iodide anions, while the smaller chloride and bromide

ions form 1:1 host-to-guest complexes.¹¹ Trimeric perfluoro-*o*-phenylenemercury coordinates halide anions in a 1:1 stoichiometric ratio of trimer/halide. The halide anions are situated above and below the cavity, providing an infinite bent polydecker with the composition $[(o-C_6F_4Hg)_3X]^-$ ($X = Cl, Br, I$) and a distorted octahedral geometry around the anion.^{10,12}

Recently, we reported the solid-state structure of a discrete, octahedrally coordinated iodide ion species sandwiched between two electroneutral trimeric *B*-hexamethyl 9-mercuracarborand-3, $[9,12-(CH_3)_2-C_2B_{10}H_8Hg]_3$, (**1**) receptors.⁸ Here we report the synthesis and structural characterization of $[I_2 \cdot X]^-$ ($X = Cl, Br, I$), unique examples of octahedrally coordinated sandwich species with the halogen atom in a formal -1 oxidation state.

Results and Discussion

Synthesis of $[I_2 \cdot X]^-$ ($X = Cl, Br, I$). The reaction of **1** with 0.5 mol equiv of halide ion salts in methylene chloride or acetone at room temperature results in the formation of $[I_2 \cdot X]^-$ sandwich complexes (Scheme 1). These anionic halide ion complexes are air- and moisture-stable solids isolated in 82–97% yields and exhibiting solubility in a variety of organic solvents (diethyl ether, acetone, acetonitrile, methylene chloride). The ¹H, ¹³C, and ¹¹B NMR spectra revealed that $[I_2 \cdot X]^-$ has a highly symmetrical structure, with chemical shifts nearly identical to those of the empty host **1**.¹³ The ¹⁹⁹Hg NMR spectrum of $[I_2 \cdot X]^-$ exhibits a downfield shift relative to **1**, which is diagnostic of guest coordination to the mercury atoms of **1**.¹³ The negative-ion fast atom bombardment (FAB) mass spectrum of $[I_2 \cdot X]^-$ exhibits an isotopic pattern expected for

(1) (a) Lee, H.; Diaz, M.; Hawthorne, M. F.; *Tetrahedron Lett.* **1999**, 40, 7651–7655. (b) Ooi, T.; Miura, T.; Maruoka, K. *Angew. Chem., Int. Ed.* **1998**, 37, 2345–2349. (c) Ooi, T.; Takahashi, M.; Maruoka, K. *J. Am. Chem. Soc.* **1996**, 118, 11307–11308. (d) Oh, T.; Lopez, P.; Reilly, M. *Eur. J. Org. Chem.* **2000**, 2901–2903.

(2) Tshinkl, M.; Schier, A.; Riede, J.; Gabbai, F. P. *Angew. Chem., Int. Ed.* **1999**, 38, 3547–3549.

(3) (a) Badr, I. H. A.; Johnson, R. D.; Diaz, M.; Hawthorne, M. F.; Bachas, L. G. *Anal. Chem.* **2000**, 72, 4249–4254. (b) Badr, I. H. A.; Diaz, M.; Hawthorne, M. F.; Bachas, L. G. *Anal. Chem.* **1999**, 71, 1371–1377.

(4) Hawthorne, M. F.; Zheng, Z. *Acc. Chem. Res.*, **1997**, 30, 267–276.

(5) Wuest, J. D. *Acc. Chem. Res.* **1999**, 32, 81–89.

(6) Tsunoda, M.; Gabbai, F. P. *J. Am. Chem. Soc.* **2000**, 122, 8335–8336.

(7) (a) Tshinkl, M.; Schier, A.; Riede, J.; Gabbai, F. P.; *Inorg. Chem.* **1997**, 36, 5706–5711. (b) Schmidtchen, F. P.; Berger, M. *Chem. Rev.* **1997**, 97, 1609–1646. (c) Beer, P. D.; Smith, D. K. In *Progress in Inorganic Chemistry*; Karlin, K. D.; Wiley: New York, 1997; Vol. 46, pp 1–97. (d) Altmann, R.; Jurkschat, K.; Schürmann, M. *Organometallics* **1998**, 17, 5858–5866.

(8) Lee, H.; Diaz, M.; Knobler, C. B.; Hawthorne, M. F. *Angew. Chem., Int. Ed.* **2000**, 39, 776–778.

(9) Shur, V. B.; Tikhonova, I. A.; Dolgushin, F. M.; Yanovsky, A. I.; Struchkov, Y. T.; Volkonsky, A. Y.; Solodova, E. V.; Panov, S. Y.; Petrovskii, P. V.; Vol'pin, M. E. *J. Organomet. Chem.* **1993**, 443, C19–C21.

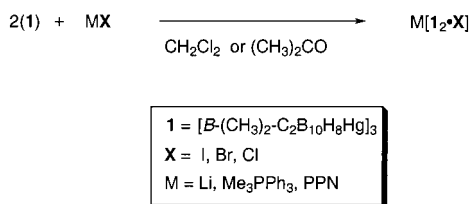
(10) Chistyakov, A. L.; Stankevich, I. V.; Gambaryan, N. P.; Struchkov, Y. T.; Yanovsky, A. I.; Tikhonova, I. A.; Shur, V. B. *J. Organomet. Chem.* **1997**, 536–537, 413–424.

(11) Yang, X.; Knobler, C. B.; Zheng, Z.; Hawthorne, M. F. *J. Am. Chem. Soc.* **1994**, 116, 7142–7159.

(12) Shur, V. B.; Tikhonova, I. A.; Yanovsky, A. I.; Struchkov, Y. T.; Petrovskii, P. V.; Panov, S. Y.; Furin, G. G.; Vol'pin, M. E. *J. Organomet. Chem.* **1991**, 418, C29–C32.

(13) Zinn, A. A.; Zheng, Z.; Knobler, C. B.; Hawthorne, M. F. *J. Am. Chem. Soc.* **1996**, 118, 70–74.

Scheme 1



$[\mathbf{1}_2\cdot\text{X}]^-$ (m/z : I = 2351, Br = 2305, Cl = 2261) and an anion envelope that corresponds to $[\mathbf{1}\cdot\text{X}]^-$ (m/z : I = 1239, Br = 1192, Cl = 1149). The dihalide complexes ($[\mathbf{1}\cdot\text{X}_2]^{2-}$, $[\text{M}(\mathbf{1}\cdot\text{X}_2)]^-$; M = Li, MePPH₃, PPN) are not observed by negative-ion FAB-MS. The $[\mathbf{1}\cdot\text{X}]^-$ species is presumed to arise from cleavage of $[\mathbf{1}_2\cdot\text{X}]^-$, since only a single sharp signal is observed in the ¹⁹⁹Hg NMR spectrum of the latter. The observation of the sandwich complexes utilizing mass spectrometry demonstrates the high stability of these anionic species.

Structure of Li[$\mathbf{1}_2\cdot\text{I}$]. The structure of $[\mathbf{1}_2\cdot\text{I}]^-$ is presented in Figures 1 and 2. Selected bond distances and angles are listed in Table 1. A single crystal of $[\text{Li}\cdot(\text{H}_2\text{O})_4][\mathbf{1}_2\cdot\text{I}]\cdot 2\text{CH}_3\text{CN}$ grown from acetonitrile/acetone crystallized in the triclinic space group *P* $\bar{1}$. The centrosymmetric trimer complex $[\mathbf{1}_2\cdot\text{I}]^-$ contains an iodide ion coordinated to six mercury atoms. The nonbonding acetonitrile molecules occupy interstices in the crystal packing, which may contribute to crystal decomposition on standing. A lithium cation, also located on an inversion center, is coordinated to the oxygen atoms of four water molecules.

The two trimeric host components of $[\mathbf{1}_2\cdot\text{I}]^-$ are inverted, parallel with respect to one another, and separated by 4.90 Å. The three mercury atoms of $[\mathbf{1}_2\cdot\text{I}]^-$ are arranged in a nearly equilateral triangle, Hg \cdots Hg = 3.6975(7)–3.7352(7) Å with Hg–Hg–Hg angles of 59.39(1)–60.39(1)° consistent with the structure of the uncomplexed host **1**.¹³ The Hg–C–C–Hg torsion angles indicate the planarity of these four atoms, with values equal to or smaller than 1°. The relatively small cavity size of **1** prevents the iodide ion from residing within the Hg–Hg–Hg plane. The iodide anion is located above the cavity center and is almost equidistant from each of the six mercury atoms (Hg–I = 3.2492(5), 3.2549(5), 3.2728(5) Å), which is less than the Hg–I van der Waals separation of 3.88 Å.^{14,15} Complex $[\mathbf{1}_2\cdot\text{I}]^-$ has shorter Hg–I distances than those found in the iodide ion complex of the cyclic perfluoro-*o*-phenylenemercury trimer mentioned above (3.331–3.487 Å)¹⁶ and the *B*-octamethyl-12-mercuracarborand-4 diiodide complex (3.438(4), 3.335(3) Å).¹⁷

The three opposing sets of Hg atoms and the central iodine atom each have a crystallographically imposed Hg–I–Hg' angle of 180°. Host **1** is a rigid tridentate chelate ligand with the mercury centers embedded within the rigid cyclic backbone. The coordination environment of Hg₃–X is mainly restricted in one dimension (via the Hg₃centroid–X–Hg₃centroid axis). Steric interaction between the opposing carborane cages and small cavity size of **1** limit Hg₃–X proximity, causing the remaining Hg–X–Hg' angles to deviate from the ideal 90° angle found in a six-coordinate of octahedral symmetry.

(14) Cauty, A. J.; Deacon, G. B. *Inorg. Chim. Acta* **1980**, *45*, L225–L227.

(15) Pauling, L. *The Nature of the Chemical Bond*, 3rd ed.; Cornell University Press: Ithaca, New York, 1960; p 260.

(16) Shur, V. B.; Tikhonova, I. A.; Yanovsky, A. I.; Struchkov, Y. T.; Petrovskii, P. V.; Panov, S. Y.; Furin, G. G.; Vol'pin, M. E. *Dokl. Akad. Nauk SSSR* **1991**, *321*, 1002–1004.

(17) Zheng, Z.; Knobler, C. B.; Mortimer, M. D.; Kong, G.; Hawthorne, M. F.; *Inorg. Chem.* **1996**, *35*, 1235–1243.

Structure of MePPH₃[$\mathbf{1}_2\cdot\text{Br}$]. The structure of $[\mathbf{1}_2\cdot\text{Br}]^-$ is presented in Figures 3 and 4. Selected bond distances and angles are listed in Table 2. A single crystal of MePPH₃[$\mathbf{1}_2\cdot\text{Br}$] $\cdot((\text{CH}_3)_2\text{CO})_2\cdot(\text{H}_2\text{O})_2$, grown from acetone, crystallized in the monoclinic space group *C2/c*. The trimer complex contains a bromide ion coordinated to six mercury atoms with the solvent molecules monocoordinated to four of the six mercury atoms, respectively. The triphenylmethylphosphonium cation is disordered about a center of symmetry with overlap of a methyl and a phenyl group.

Bromide ion is located on a 2-fold axis between two trimeric hosts and is coordinated to all six Hg atoms. The Hg–Br distances (3.132(1)–3.309(1) Å) are within the van der Waals separation of 3.68 Å.^{14,15} These distances are comparable with those in previously reported Hg–Br complexes: trimeric perfluoro-1,2-phenylenemercury has Hg–Br distances ranging from 3.07 to 3.39 Å,¹⁸ and tetrameric mercuracarborand Hg–Br distances range from 3.028 to 3.087 Å.^{11,13} The two trimeric host components of $[\mathbf{1}_2\cdot\text{Br}]^-$ are related by a 2-fold symmetry axis and are nearly parallel to one another. The separation measured between midpoints of each of the two Hg₃ planes is 4.764 Å. The opposing Hg atoms and central bromine atom have near linear Hg–Br–Hg' angles of 177.72(4) and 176.13(5)°.

Each acetone and water molecule coordinates with a discrete mercury center (Hg2 \cdots O1S 2.79(1), Hg3 \cdots O1T 2.93(4) Å, respectively) and the Hg \cdots O distances are within the sum of the van der Waals separation of 3.13 Å.^{14,15} The Hg1 center is not observed to be coordinated to solvent. Using the Hg1–Br distance as a reference (3.186(1) Å), the coordination of an acetone molecule to Hg2 appears to weaken the resulting Hg2–Br bond (3.309(1) Å). Acetone has a shorter Hg–O distance and a greater influence on the resulting Hg–Br bond than does the water molecule (Hg3–Br 3.132(1) Å). In previously reported tetrameric mercuracarborand halide complexes, each mercury atom is coordinated to the halide ion and no competing solvent molecules bind to mercury.¹¹ However, the tetrameric complexes were crystallized in a coordinating solvent such as acetone, diethyl ether, or acetonitrile. Attempts to obtain single crystals of $[\mathbf{1}_2\cdot\text{Br}]^-$ from weakly coordinating solvents such as methylene chloride or toluene were unsuccessful.

The three mercury atoms in $[\mathbf{1}_2\cdot\text{Br}]^-$ are arranged in a near equilateral triangle (Hg \cdots Hg 3.690(1)–3.770(1) Å; Hg–Hg–Hg 59.04(2)–61.17(1)°). The three Hg atoms must be coplanar, but the Hg–C–C–Hg torsion angles deviate from linearity, 0(1)–4(1)°, contrasting with those reported for the empty host **1** (equal to or smaller than 1°).¹³ The Hg–Br interactions and steric hindrance of the opposing icosahedra contribute to the observed deviation from linearity of the C–Hg–C angles (168.0(4)–172.6(4)°) relative to those of the uncomplexed host **1** (172.7(6)–174.9(6)°).¹³

Structure of PPN[$\mathbf{1}_2\cdot\text{Cl}$]. The structure of $[\mathbf{1}_2\cdot\text{Cl}]^-$ is presented in Figures 5 and 6. Selected bond distances and angles are listed in Table 3. A single crystal of PPN[$\mathbf{1}_2\cdot\text{Cl}$], grown from acetone/acetonitrile, crystallized in the monoclinic space group *C2/m*. The trimer complex contains a chloride ion coordinated to six mercury atoms of $[\mathbf{1}_2\cdot\text{Cl}]^-$. Each of the two crystallographically unrelated mercuracarborands, **1**, in $[\mathbf{1}_2\cdot\text{Cl}]^-$ has mirror symmetry.

One of the two trimeric hosts of $[\mathbf{1}_2\cdot\text{Cl}]^-$ is inverted with respect to the other host and they are nearly parallel with a separation of 4.672 Å. The chloride ion lies 2.344(6) and 2.328(6) Å from the Hg₃ planes and is almost equidistant from

(18) Shur, V. B.; Tikhonova, I. A.; Yanovsky, A. I.; Struchkov, Y. T.; Petrovskii, P. V.; Panov, S. Y.; Furin, G. G.; Vol'pin, M. E. *Izv. Akad. Nauk SSSR, Ser. Khim.* **1991**, *2*, 1466–1467.

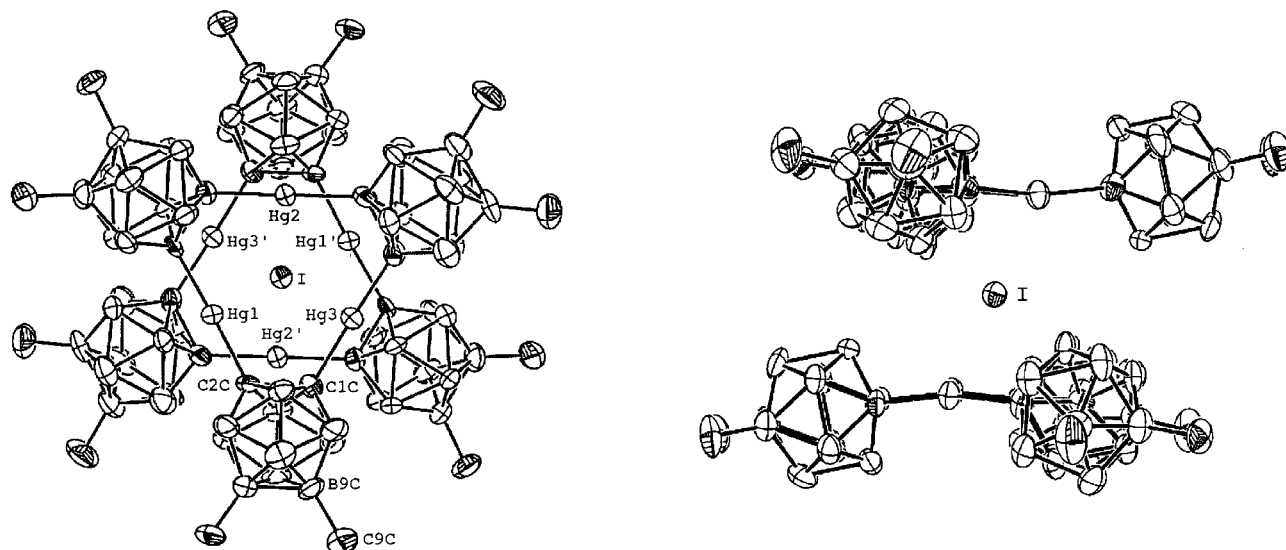


Figure 1. Structure of $[I_2 \cdot I]^-$ (ORTEP plot; hydrogen atoms omitted for clarity).

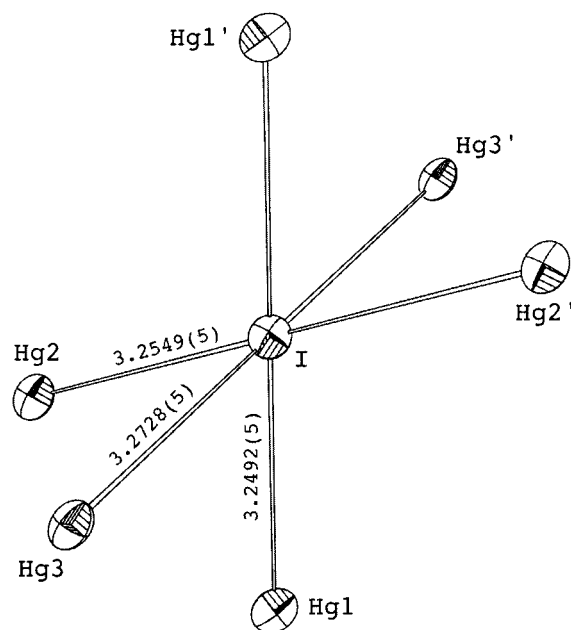


Figure 2. Coordination environment of iodide ion in $[I_2 \cdot I]^-$ (ORTEP plot; carbon, boron, and hydrogen atoms omitted for clarity; bond lengths in Å).

each of the six mercury atoms ($Hg-Cl = 3.146(6)$ – $3.177(5)$ Å); distances are within the van der Waals separation of 3.53 Å.^{14,15} For comparison, the reported structure of the 1:2 adduct of chloride ion with 1,2-diphenylenedimercury dichloride has two $Hg-Cl$ distances of 2.925 and 3.167 Å.¹⁹ The pentacoordinated chloride complex, $[(CF_3)_2CHg]_5 \cdot Cl_2^{2-}$, has $Hg-Cl$ distances ranging from 3.089 to 3.388 Å,⁹ and cyclic 12-mercuracarborand-4 forms a 1:1 complex with chloride ion with a $Hg-Cl$ distance of 2.944 Å.¹¹ The opposing Hg atoms and central chloride atom have linear $Hg-Cl-Hg'$ angles of $179.5(2)$ and $179.7(2)^\circ$.

In simplest terms, the coordination of the halide ion in $[I_2 \cdot X]^-$ ($X = I, Br, Cl$) must arise from the interaction of the filled p-orbitals of the halide anion with the empty mercury p-orbitals having the proper orientation to form three $p_{Hg}-p_X-p_{Hg}$ three-center two-electron bonds and a sandwich structure (Chart 1).

(19) Beauchamp, A. L.; Olivier, M. J.; Wuest, J. D.; Zacharie, B. *J. Am. Chem. Soc.* **1986**, *108*, 73–77.

Table 1. Selected Bond Distances (Å) and Angles (deg) for Compound $[I_2 \cdot I]^-$

Distances (Å)			
Hg1–C1A	2.06(1)	Hg1–I	3.25
Hg1–C2C	2.12(1)	Hg2–I	3.25
Hg2–C2A	2.10(1)	Hg3–I	3.27
Hg2–C1B	2.11(1)	Hg1··Hg2	3.728(1)
Hg3–C2B	2.08(1)	Hg1··Hg3	3.697(1)
Hg3–C1C	2.08(1)	Hg2··Hg3	3.735(1)
Angles (deg)			
C1A–Hg1–C2C	169.0(5)	Hg1–I–Hg2	69.95(1)
C2A–Hg2–C1B	171.0(5)	Hg1–I–Hg3	69.07(1)
C2B–Hg3–C1C	169.4(5)	Hg2–I–Hg3	69.81(1)
Hg1–Hg2–Hg3	59.4(1)	Hg1–I–Hg1'	180
Hg2–Hg3–Hg1	60.2(1)	Hg1–I–Hg2'	110.05(1)
Hg3–Hg1–Hg2	60.4(1)	Hg1–I–Hg3'	110.93(1)
Hg1–C1A–C2A–Hg2	–1(1)	Hg2–I–Hg2'	180
Hg2–C1B–C2B–Hg3	1(1)	Hg2–I–Hg3'	110.19(1)
Hg3–C1C–C2C–Hg1	–1(1)	Hg3–I–Hg3'	180

Mercury-199 NMR Investigation of Halide Ion Complexation by $[(CH_3)_2C_2B_{10}H_8Hg]_3$. The ^{199}Hg nucleus has a spin quantum number of $I = 1/2$ and a moderately large natural abundance (16.9%). The extreme sensitivity of ^{199}Hg NMR chemical shifts to their immediate environment²⁰ makes ^{199}Hg NMR spectroscopy a very useful probe for observing host–guest interactions,¹¹ especially since mercuracarborands and their corresponding anion complexes have very similar ^{13}C , ^{11}B , and 1H NMR spectra.^{4,8,11}

The ^{199}Hg NMR data of **1** and its halide complexes are listed in Table 4. Halide ion coordination to **1** results in resonances corresponding to $[I_2 \cdot Cl]^-$ ($\delta = -1117$), $[I_2 \cdot Br]^-$ ($\delta = -1082$), and $[I_2 \cdot I]^-$ ($\delta = -957$), respectively. Halide ion complexes of **1** have ^{199}Hg NMR chemical shifts that are essentially independent of solvent and concentration at room temperature with resonance peaks remaining relatively sharp, suggesting the existence of a single species. The shielding effect of halide ions covalently bonded to mercury atoms of **1**, $I > Br > Cl$, is consistent with the trend observed with cyclic tetrameric 12-mercuracarborand-4 halide complexes.¹¹

Conversion of **1 to $[I_2 \cdot X]^-$ ($X = Cl, Br$) Monitored by ^{199}Hg NMR Spectroscopy.** The ^{199}Hg NMR resonances of $[I_2 \cdot X]^-$ ($X = Cl, Br$) were measured in methylene chloride due to the solubility and relatively weak coordinating properties of

(20) Maciel, G. E.; Borzo, M. *J. Magn. Reson.* **1973**, *10*, 388–390.

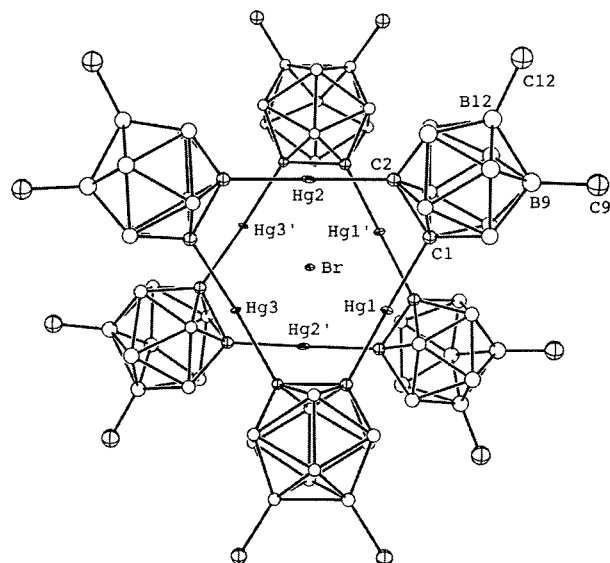


Figure 3. Structure of $[1_2 \cdot Br]^-$ (ORTEP plot; hydrogen atoms omitted for clarity).

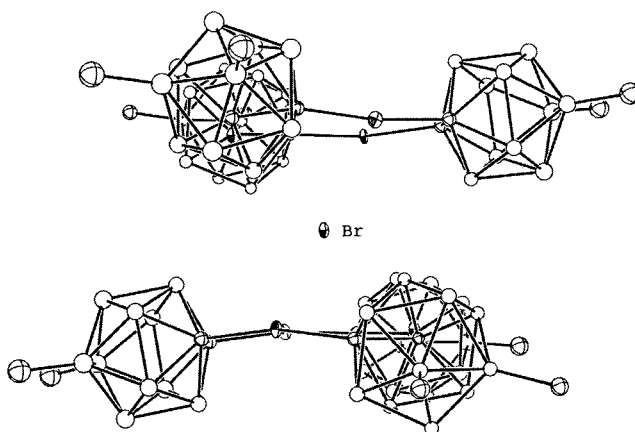


Figure 4. Coordination environment of bromide ion in $[1_2 \cdot Br]^-$ (ORTEP plot; carbon, boron, and hydrogen atoms omitted for clarity; bond lengths in Å).

Table 2. Selected Bond Distances (Å) and Angles (deg) for Compound $[1_2 \cdot Br]^-$

Distances (Å)			
Hg1–Br	3.186(1)	Hg2–C1B	2.09(1)
Hg2–Br	3.309(1)	Hg3–C1C	2.09(1)
Hg3–Br	3.132(1)	Hg3–C2B	2.10(1)
Hg2–O1S	2.79(1)	Hg1–C2C	2.08(1)
Hg3–O1T	2.94(3)	Hg1–C1A	2.09(1)
Hg1···Hg2	3.690(1)	Hg2–C2A	2.09(1)
Hg2···Hg3	3.770(1)	Hg3···Hg1	3.719(1)
Angles (deg)			
C(2C)–Hg(1)–C(1A)	170.8(4)	Hg1–Br–Hg3	72.11(3)
C(2A)–Hg(2)–C(1B)	172.6(4)	Hg1–Br–Hg1'	110.09(5)
C(1C)–Hg(3)–C(2B)	168.0(4)	Hg1–Br–Hg2'	108.43(2)
Hg1–Hg2–Hg3	59.79(2)	Hg1–Br–Hg3'	177.72(4)
Hg2–Hg3–Hg1	59.04(2)	Hg2–Br–Hg3	71.59(2)
Hg3–Hg1–Hg2	61.17(1)	Hg2–Br–Hg2'	176.13(5)
Hg1–Br–Hg2	69.21(2)	Hg2–Br–Hg3'	110.89(2)
Hg3–Br–Hg3'	105.70(5)	Br–Hg2–O1S	138.8(3)

this solvent. The stepwise addition of MePPh₃Br or PPnCl to a methylene chloride solution of **1** results in the formation of discrete sets of resonances observed by ¹⁹⁹Hg NMR spectro-

scopy at room temperature. Similar titration experiments carried out in acetone solution with **1** and LiI gave results identical to those reported below with Br[−] and Cl[−] complexes of **1**. The $[1_2 \cdot I]^-$ complex persisted at $\delta = -957$ in the presence of a 5 molar excess of LiI. These results were not reported in the original communication.⁸

Incremental addition of a methylene chloride solution of MePPh₃Br (¹/₄ equiv) to **1** in the same solvent results in sharp resonances at $\delta = -1082$ and -1225 (Figure 7). After an additional ¹/₄ equiv, only a single sharp resonance at $\delta = -1082$ is observed and the resonance correlating to **1** ($\delta = -1224$) is no longer observed. Further addition of up to 5 molar equiv of Me₃PPh₃Br resulted in no observable change in the ¹⁹⁹Hg NMR spectrum, suggesting that the resonance at $\delta = -1082$ corresponds to the $[1_2 \cdot Br]^-$ species.

Incremental addition of a methylene chloride solution of PPnCl (¹/₄ equiv) to a methylene chloride solution of **1** resulted in sharp resonances at $\delta = -1117$ and -1224 (Figure 8). After an additional ¹/₄ equiv, only a single sharp resonance at $\delta = -1117$ was observed. When up to 5 molar equiv of PPnCl was added to the CH₂Cl₂ solution of **1**, no further change in the spectrum was observed. These results suggest that the resonance at $\delta = -1117$ corresponds to a $[1_2 \cdot Cl]^-$ species.

The ¹⁹⁹Hg NMR spectrometric data are consistent with the X-ray structures of $[1_2 \cdot I]^-$, $[1_2 \cdot Br]^-$, and $[1_2 \cdot Cl]^-$, which suggests a 2:1 trimer host (**1**) to halide ion ratio and that the solid-state species persist in solution. The $[1_2 \cdot X]^-$ species are relatively stable and observed in the negative FAB mass spectrum ($[1_2 \cdot I]^-$, $m/z = 2351$; $[1_2 \cdot Br]^-$, $m/z = 2305$; $[1_2 \cdot Cl]^-$, $m/z = 2261$). The corresponding $[1 \cdot X]^-$ ions produced by dissociation in the mass spectrometer appear at $m/z = 1239$, 1192, and 1149, respectively. The $[1_2 \cdot I]^-$ and $[1 \cdot I]^-$ data were previously reported.⁸

Experimental Section

General Considerations. All solvents were reagent grade. Deuterated solvents were obtained from Cambridge Isotope Laboratories. Methyltriphenylphosphonium bromide, bis(triphenylphosphoranylidene)ammonium chloride (PPnCl), and lithium iodide were obtained from Aldrich and used without further purification. Compound **1** was prepared according to literature methods.¹³

Physical Measurements. The ¹H and ¹³C spectra were recorded with Bruker AM 400 and 500 spectrometers. The ¹¹B spectra were obtained with an AM 500 spectrometer. Chemical shifts for ¹H and ¹³C NMR

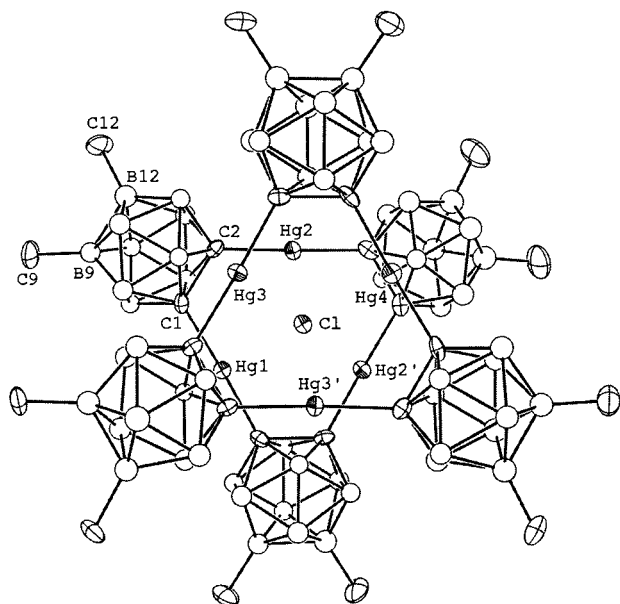


Figure 5. Structure of $[I_2 \cdot Cl]^-$ (ORTEP plot; hydrogen atoms omitted for clarity).

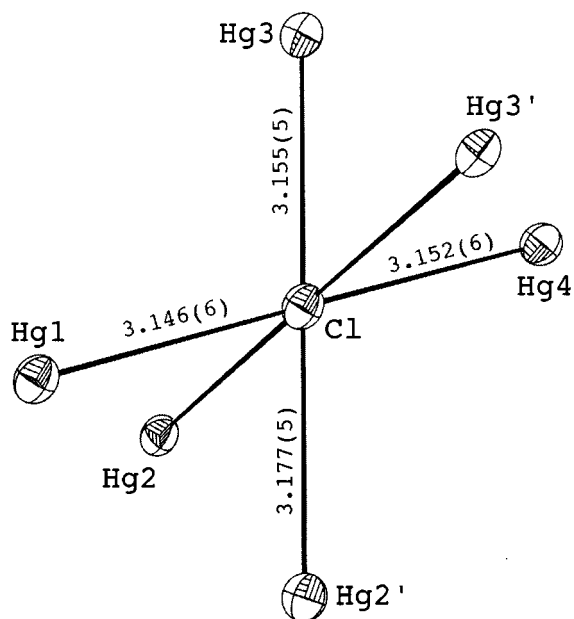
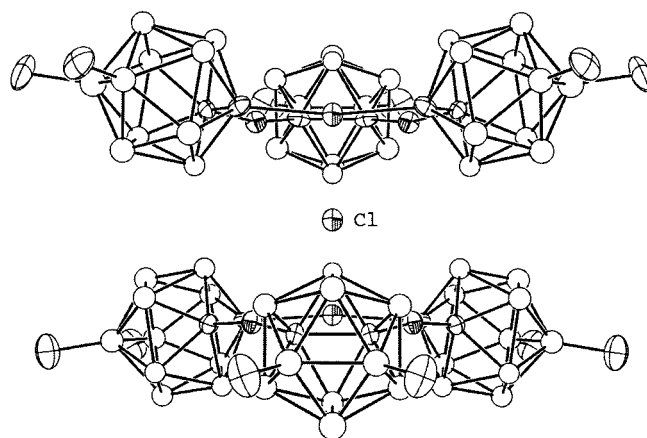


Figure 6. Coordination environment of chloride ion in $[I_2 \cdot Cl]^-$ (ORTEP plot; carbon, boron, and hydrogen atoms omitted for clarity; bond lengths in Å).

spectra were referenced to the residual protons and carbon atoms present in deuterated solvents. Chemical shift values for ^{11}B spectra were referenced relative to external $BF_3 \cdot OEt_2$ (δ 0.0 ppm with negative δ values upfield). The $^{199}Hg\{^1H\}$ NMR spectra were recorded at 25 °C with a Bruker 500 spectrometer at 89.6 MHz by using broad-band decoupling. External 0.5 M $PhHgCl$ in $DMSO-d_6$ solution was used as the reference at -1187 ppm relative to neat Me_2Hg .²¹ All FAB mass spectra were obtained on VG-ZAB.

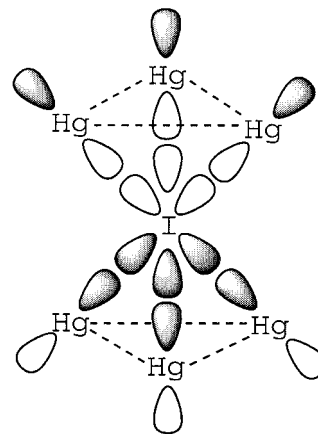
Li $[I_2 \cdot I]$. Species **1**¹³ (0.50 g, 0.45 mmol) in acetone (40 mL) was treated with LiI (0.15 g, 1.12 mmol) at room temperature for 12 h. The solvent was removed under vacuum, and the residual solid was washed with water and then extracted with three 25-mL portions of diethyl ether. The combined organic phase was dried over anhydrous magnesium sulfate and filtered. The solvent was removed under vacuum to give $Li[I_2 \cdot I]$ in 82% yield. Crystals of $[Li(H_2O)_4][I_2 \cdot I] \cdot 2(CH_3CN)$ suitable for X-ray diffraction studies form after repeated recrystallization

(21) Sens, M. A.; Wilson, N. K.; Ellis, P. D.; Odom, J. D. *J. Magn. Reson.* **1975**, *19*, 323–336.

Table 3. Selected Bond Distances (Å) and Angles (deg) for Compound $[I_2 \cdot Cl]^-$

Distances (Å)			
Hg1–Cl	3.146(6)	Hg1–ClA	2.07(2)
Hg2–Cl	3.177(5)	Hg2–ClB	2.07(2)
Hg3–Cl	3.155(5)	Hg2–C2A	2.05(2)
Hg4–Cl	3.152(6)	Hg3–C1C	2.07(2)
Hg1–Hg2	3.702(2)	Hg3–C1D	2.09(2)
Hg2–Hg2'	3.657(2)	Hg4–C2C	2.11(2)
Hg3–Hg4'	3.702(2)	Hg3–Hg3'	3.651(2)
Angles (deg)			
C1A–Hg1–ClA'	170.1(9)	Hg1–Cl–Hg3	108.5(2)
C2A–Hg2–ClB	170.0(6)	Hg1–Cl–Hg4	179.5(2)
Hg1–Hg2–Hg2'	60.40(2)	Hg2–Cl–Hg3	109.51(3)
Hg2–Hg1–Hg2'	59.19(4)	Hg2–Cl–Hg4	107.9(2)
Hg3–Hg4–Hg3'	59.10(4)	Hg2–Cl–Hg3'	179.7(2)
Hg4–Hg3–Hg3'	60.45(2)	Hg3–Cl–Hg4	71.9(1)
Hg1–Cl–Hg2	71.7(1)	Hg3–Cl–Hg3'	70.7(1)
Hg2–Cl–Hg2'	70.3(1)		

Chart 1

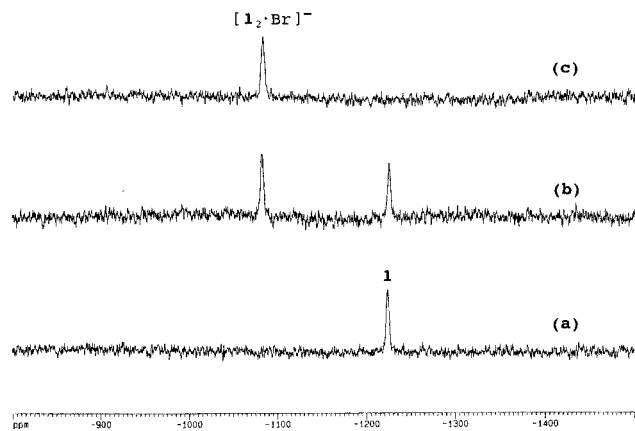
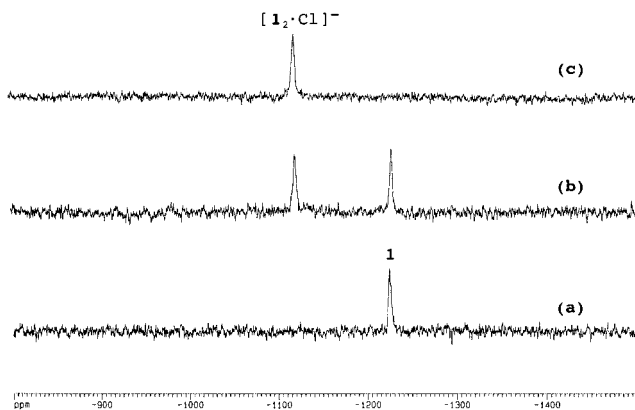


from CH_3CN /acetone; mp >300 °C. $Li[I_2 \cdot I]$: 1H NMR (400 MHz, acetone- d_6 , 25 °C) δ 3.0–1.0 (B–H), 0.05 (CH_3); $^{13}C\{^1H\}$ NMR (90 MHz, acetone- d_6 , 25 °C) δ 89.4 (carborane-C), 0.81 (br s, CH_3); $^{11}B\{^1H\}$ NMR (160 MHz, acetone, 25 °C, $BF_3 \cdot Et_2O$ external) δ 10.7, -3.3 , -8.0 (2:2:6); $^{199}Hg\{^1H\}$ NMR (89.6 MHz, acetone, 25 °C, external 1.0 M $PhHgCl$ in $DMSO-d_6$; chemical shift δ -1187 ²¹ upfield from neat Me_2Hg) δ -957 ; negative-ion FAB-MS, m/z (%) 2351 (5) $[I_2 \cdot I]^-$, 1239 (100) $[I \cdot I]^-$.

Table 4. ^{199}Hg NMR Shifts of *B*-Hexamethyl-9-mercurocarborand-3 (**1**) and the Halide Ion Complexes at 25 °C

Compound	Chemical Shift (δ)
1 ^a	-1224
[1 \cdot Cl] PPN ^a	-1117
[1 \cdot Br] MePPh ₃ ^a	-1082
[1 \cdot I] Li ^b	-957

^a Measured in CH_2Cl_2 ^b Measured in acetone. See Experimental Section for details.

**Figure 7.** A ^{199}Hg NMR study on the addition of MePPh₃Br to an 18 mM CH_2Cl_2 solution of **1** with MePPh₃Br/**1** ratios of (a) 0.0, (b) 0.25, and (c) 0.50.**Figure 8.** A ^{199}Hg NMR study on the addition of PPNCl to an 18 mM CH_2Cl_2 solution of **1** with PPNCl/**1** ratios of (a) 0.0, (b) 0.25, and (c) 0.50.

MePPh₃[1** \cdot Br].** To a methylene chloride solution (1.5 mL) of **1**¹³ (30 mg, 27 μmol), MePPh₃Br (4.8 mg, 13.5 μmol) was added. The solvent was removed to give a white solid which upon recrystallization from acetone afforded a quantitative yield of MePPh₃[**1** \cdot Br] (97%): ^1H NMR (400 MHz, acetone-*d*₆, 25 °C) δ 7.85 (m, 20H), 3.20 (3H, Me, $J_{\text{C-P}} = 14.13$ Hz), 3.0–1.5 (B–H), 0.06 (B–CH₃); $^{13}\text{C}\{^1\text{H}\}$ NMR (100 MHz, acetone-*d*₆, 25 °C) δ 136.0 (d ph, $J_{\text{C-P}} = 2.9$ Hz), 134.2 (d, ph, $J_{\text{C-P}} = 10.8$ Hz), 131.1 (d, ph, $J_{\text{C-P}} = 12.9$ Hz), 120.7 (d, ph, $J_{\text{C-P}} = 89.1$ Hz), 87.2 (carborane-C), 8.7 (d, Me, $J_{\text{C-P}} = 57.3$ Hz); $^{31}\text{P}\{^1\text{H}\}$ NMR (160 MHz, acetone-*d*₆, 25 °C, external (CH₃O)P in benzene-*d*₆; chemical shift δ 36.2²² downfield from 85% H₃PO₄) δ 22.10 (d, $J_{\text{PC}} = 2.4$ Hz); $^{11}\text{B}\{^1\text{H}\}$ NMR (160 MHz, acetone, 25 °C, BF₃·Et₂O external) δ 9.8, -4.3, -9.1, -11.1 (2:2:6); $^{199}\text{Hg}\{^1\text{H}\}$ NMR (89.6 MHz, CH_2Cl_2 , 25 °C, external 0.5 M PhHgCl in DMSO-*d*₆; chemical shift δ -1187²¹ upfield from neat Me₂Hg) δ -1082; negative-ion FAB-MS m/z (%) 2305 (15) [**1** \cdot Br]⁻, 1192 (100) [**1** \cdot Br]⁻.

PPN[1** \cdot Cl].** To a methylene chloride solution (1.5 mL) of **1**¹³ (30 mg, 27 μmol), PPNCl (7.8 mg, 13.5 μmol) was added. The solvent

(22) *Bruker Almanac 1991*; Thieme-Verlag: Stuttgart, Germany, 1990; p 83.

was removed to give a white solid and upon recrystallization from acetone afforded a quantitative yield of PPN[**1** \cdot Cl] (97%): ^1H NMR (400 MHz, acetone-*d*₆, 25 °C) δ 7.70 (m, 12H), 7.57 (m, 8H), 3.0–1.5 (B–H), 0.07 (B–CH₃); $^{13}\text{C}\{^1\text{H}\}$ NMR (100 MHz, acetone-*d*₆, 25 °C) δ 134.5 (ph), 133.2 (m, ph), 128.8 (br s, ph), 86.8 (carborane-C); $^{31}\text{P}\{^1\text{H}\}$ NMR (160 MHz, acetone-*d*₆, 25 °C, external (CH₃O)P in benzene-*d*₆, chemical shift δ 36.2²² downfield from 85% H₃PO₄) δ 20.90; $^{11}\text{B}\{^1\text{H}\}$ NMR (160 MHz, acetone, 25 °C, BF₃·Et₂O external) δ 9.8, -4.3, -9.1, -11.6 (2:2:6); $^{199}\text{Hg}\{^1\text{H}\}$ NMR (89.6 MHz, CH_2Cl_2 , 25 °C, external 0.5 M PhHgCl in DMSO-*d*₆; chemical shift δ -1187²¹ upfield from neat Me₂Hg) δ -1117; negative-ion FAB-MS, m/z (%) 2261 (15) [**1** \cdot Cl]⁻, 1149 (100) [**1** \cdot Cl]⁻.

Titration of **1 with MePPh₃Br.** In a 10-mm NMR tube, **1** (30 mg, 27 μmol) was dissolved in CH_2Cl_2 (1.5 mL). A CH_2Cl_2 (2.0 mL) solution of MePPh₃Br (19 mg, 54 μmol , 27 mM) was added to **1** in increments of 0.25 equiv (0.25 mL, 6.8 μmol). After each increment of the MePPh₃Br salt was added, the mixture was mixed well and the ^{199}Hg NMR spectrum recorded. The procedure was repeated until no further change in the spectrum was observed.

Titration of **1 with PPNCl.** Procedure is the same as above, with the exception of PPNCl (31 mg, 54 μmol , 27 mM).

Solution and Refinement of Crystal Structures. Collection and Reduction of X-ray Data for [Li·(H₂O)₄][1** \cdot I]·2CH₃CN.** A colorless crystal, obtained from a THF/CH₃CN solution, was placed in a capillary and mounted on a Huber (Crystal Logic) diffractometer. Unit cell parameters were determined from a least-squares fit of 47 accurately centered reflections ($9.9 < 2\theta < 20.5^\circ$). These dimensions and other parameters, including conditions of data collection, are summarized in Table 5. Data were collected at 25 °C in the θ - 2θ scan mode. Three intense reflections (0 3 0, 4 0 1, 2 4 5) were monitored every 100 reflections to check stability. Intensities of these reflections decayed 1.1% during the course of the experiment (169.8 h). Of the 13 199 unique reflections measured, 6469 were considered observed ($I > 2\sigma(I)$) and were used in the subsequent structure analysis. Data were corrected for Lorentz and polarization effects and for absorption and secondary extinction. Programs used in this work include locally modified versions of the following programs: CARESS (Broach, Coppens, Becker, and Blessing), peak profile analysis, Lorentz and polarization corrections; ORFLS (Busing, Martin, and Levy), structure factor calculation and full-matrix least-squares refinement, SHELX76 (Sheldrick), a crystal structure package, SHELX86 (Sheldrick), a crystal structure solution package, and ORTEP (Johnson).

Solution and Refinement of the Structure of [Li·(H₂O)₄][1** \cdot I]·2CH₃CN.** Atoms were located by use of heavy atom methods. All calculations were performed on a VAX 3100 computer in the J. D. McCullough X-ray Crystallography Laboratory. With the exception of Li, all non-hydrogen atoms were refined with anisotropic parameters. All H were included in structure factor calculations, but parameters were not refined. H atoms were assigned isotropic displacement values based approximately on the value for the attached atom. Scattering factors for H were obtained from Stewart et al.²³ and for other atoms were taken from *The International Tables for X-ray Crystallography*.²⁴ The largest peak maximum and minimum on a final difference electron density map were 2.34 (near Hg) and -1.72 e \AA^{-3} .

Collection and Reduction of X-ray Data for MePPh₃P[1** \cdot Br]·((CH₃)₂CO)₂·(H₂O)₂.** A colorless cut parallelepiped obtained from an acetone solution was mounted on a thin glass fiber on a Bruker SMART ccd diffractometer. Unit cell parameters were determined from a least-squares fit of 1001 reflections ($6.91 < 2\theta < 56.33^\circ$). These dimensions and other parameters, including conditions of data collection, are summarized in Table 5. Data were collected at 100 K. Intensities did not decay during the course of the experiment. Of the 12 824 unique reflections measured, 9789 were considered observed ($I > 2\sigma(I)$) but all reflections were used in the subsequent structure analysis. Data were corrected for Lorentz and polarization effects and for absorption. Programs used in this work are those supplied with the Bruker SMART ccd diffractometer.

(23) Stewart, R. F.; Davidson, E. R.; Simpson, W. T. *J. Chem. Phys.* **1965**, *42*, 3175.

(24) *International Tables for X-ray Crystallography*; Kynoch Press: Birmingham, England, 1974; Vol. IV.

Table 5. Crystallographic Data Collection for Li[1₂·I], MePh₃P[1₂·Br], and PPN[1₂·Cl]

	Li·(H ₂ O) ₄ [1 ₂ ·I]·2CH ₃ CN	MePh ₃ P[1 ₂ ·Br]·2H ₂ O·2((CH ₃) ₂ CO)	PPN[1 ₂ ·Cl]
formula	C ₂₈ H ₉₈ B ₆₀ Hg ₆ LiN ₂ O ₄	C _{24.5} H _{56.5} B ₃₀ Br ₅ Hg ₃ O _{1.5} P _{0.5}	C ₆₀ H ₁₁₄ B ₆₀ ClH ₆ NP ₂
fw	2513.06	1356.71	2799.05
cryst syst	triclinic	monoclinic	monoclinic
space group	P1̄	C2/c	C2/m
color of cryst	colorless	colorless	colorless
cryst dimens, (mm)	0.2 × 0.2 × 0.5	0.5 × 0.5 × 0.5	0.35 × 0.1 × 0.05
a, (Å)	13.312(8)	24.671(8)	37.27(2)
b, (Å)	13.983(9)	17.576(6)	29.25(1)
c, (Å)	13.996(9)	26.079(8)	10.990(4)
α, (deg)	61.16(2)	90	90
β, (deg)	82.34(2)	106.424(6)	100.659(7)
γ, (deg)	86.58(2)	90	90
V, (Å ³)	4365(2)	10847(6)	11774(8)
Z	1	8	4
ρ _{calcd.} , (g cm ⁻³)	1.84	1.662	1.579
temp, K	298	373(2)	298(2)
radiation, λ (Å)	Mo Kα (0.7107)	Mo Kα (0.7107)	Mo Kα (0.7107)
μ, cm ⁻¹	105.2	8.878	7.877
no. unique reflcns	13 199	34 317	37 753
no. obsd reflcns	6469	12 824	14 338
No. params refined	502	353	484
R _w ^a , R _w ^b	0.063, 0.171	0.0607, 0.1506	0.0911, 0.2369
GOF ^c	1.02	1.075	1.022

^a $R = S||F_o| - |F_c||/|F_o|$. ^b $R_w = [\sum w(|F_o| - |F_c|)^2 / \sum w|F_o|^2]^{1/2}$. ^c $GOF = [\sum w(|F_o| - |F_c|)^2 / (N_o - N_v)]^{1/2}$, where $w = 1/(\sigma^2|F_o|)$.

Solution and Refinement of the Structure of MePh₃P[1₂·Br]·(CH₃)₂CO₂·(H₂O)₂. Atoms were located by use of statistical methods. The asymmetric unit includes a Hg trimer, one molecule of acetone, one-half molecule of water, one-half cation, and one-half atom of Br. The Br atom lies on a 2-fold axis. The methyltriphenylphosphonium cation is disordered about a center of symmetry with overlap of one methyl group and one phenyl group. With the exception of the icosahedral C₂B₁₀ atoms, all nonhydrogen atoms were included with anisotropic displacement parameters. Hydrogen atoms of water and of the disordered methyl group were not located. All other hydrogen atoms were included in calculated positions in the refinement. The isotropic displacement parameters for hydrogen atoms were based on the values for the attached atoms. Scattering factors for H were obtained from Stewart et al.²³ and for other atoms were taken from *The International Tables for X-ray Crystallography*.²⁴ The maximum and minimum values on a final difference electron density map were 4.11 and -2.75 e Å⁻³.

Collection and Reduction of X-ray Data for Compound PPN-[1₂·Cl]. A colorless crystal, obtained from a CH₃CN/acetone solution, was mounted on a fiber and placed on a Bruker SMART ccd diffractometer. Cell dimensions, obtained from 1016 reflections (6.68 < 2θ < 56.48°) and other parameters, including conditions of data collection, are summarized in Table 5. Data were collected at 25 °C. The first 50 frames were collected again at the end of the measurement

to check stability. There was no decay during the course of the experiment. Of the 14 338 unique reflections measured, 8057 were considered observed ($I > 2\sigma(I)$). All reflections were used in the subsequent structure analysis. Data were corrected for Lorentz and polarization effects and for secondary extinction and absorption. Programs used in this work include SMART, SAINT, and SHELXTL, all supplied by Bruker for the SMART system.

Solution and Refinement of the Structure of Compound PPN-[1₂·Cl]. Atoms were located by use of direct methods. With the exception of boron, all non-hydrogen atoms were refined anisotropically. All H were placed in calculated positions. H atoms were assigned isotropic displacement values based approximately on the value for the attached atom. Scattering factors for H were obtained from Stewart et al.²³ and for other atoms were taken from *The International Tables for X-ray Crystallography*.²⁴ The largest peaks on a final difference electron density map were 3.93 and -5.81 e Å⁻³. Anomalous dispersion terms were included for Cl.

Acknowledgment. We are grateful to the National Science Foundation (Grant CHE-9730006 and Equipment Grant CHE-9871332) for their support of this research.

JA010755L